Changing spectral patterns of long-term drought propensity in Iran through reliability–resilience–vulnerability-based Drought Management Index

Peyman Mahmoudi[1] | Rajib Maity[2] | Seyed Mahdi Amir Jahanshahi[3] | Kironmala Chanda[4]

[1]Department of Physical Geography, Faculty of Geography and Environmental Planning, University of Sistan and Baluchestan, Zahedan, Iran

[2]Department of Civil Engineering, Indian Institute of Technology Kharagpur, Kharagpur, India

[3]Department of Statistics, Faculty of Mathematics, Statistics and Computer Science, University of Sistan and Baluchestan, Zahedan, Iran

[4]Department of Civil Engineering, Indian Institute of Technology (ISM), Dhanbad, India

Correspondence
Peyman Mahmoudi, Department of Physical Geography, Faculty of Geography and Environmental Planning, University of Sistan and Baluchestan, Zahedan, Iran.
Email: p_mahmoudi@gep.usb.ac.ir

Abstract

This study aims to investigate the change in spectral patterns of droughts in Iran based on the concepts of reliability, resilience, and vulnerability (RRV) in the context of time. To achieve this goal, RRV values were first estimated based on monthly gridded soil moisture data for a period of 64 years (1955–2018) for the framework of Iran's political borders. The pairwise comparison of the values of the three variables RRV indicates a positive relationship between reliability–resilience and a negative relationship between reliability–vulnerability and resilience–vulnerability. In order to obtain the Joint Probability Distribution between reliability–vulnerability, Drought Management Index (DMI) for all the gridded points within Iran's political borders were calculated by fitting the Gaussian copula. According to this index, drought is an unfavourable climatic phenomenon that is associated with increased Vulnerability and decreased Reliability. The temporal and spatial changes of this index indicate that DMI values are always high for the south, east and centre of Iran and low for the western and northern half. To study the change in spectral patterns of droughts in Iran, the 64-year period studied (1955–2018) was divided into two equal periods of 32 years. Then, using spectral analysis through Fourier transform method, the first three periodicities related to each period that had the highest powers were extracted. Finally, their periodicity was compared. The results indicated that the drought periodicities in the north-west, north-east, west, south-west, and south of Iran have become longer, that is, their nature has been changed from shorter periodicities to longer ones. This change of nature in their first three periodicities has been sometimes from 2–10 years to 2–15 years, from 2–10 years to 3–30 years, and from 3–8 years to 8–15 years. However, the periodicities of droughts in the eastern, south-eastern, and central Iran has changed from longer periodicities to shorter ones. It has been changed from 3–15 years to 2–6 years, from 3–15 years to 2–3 years, and from 3–30 years to 3–15 years.

KEYWORDS
climate change, Drought Management Index (DMI), Gaussian copula, joint probability distribution, reliability, resilience, soil moisture, vulnerability

1 | INTRODUCTION

The vast country of Iran with a rainfall of about one-third of the world rainfall is located in one of the arid and semiarid regions of the world and drought is one of the main features and characteristics of its climate (Vaghefi *et al.*, 2019; Kaboli *et al.*, 2021). In recent years, for the reasons that are often related to global climate change, precipitation anomalies have increased in various parts of Iran, and severe spatial and temporal fluctuations of drought have caused enormous damage to the Iranian economy. (Mahmoudi and Daneshmand, 2018). Decreased rangeland yield (Joneidi *et al.*, 2020), reduced crop production especially rainfed (Shean, 2008), reduced agricultural and drinking water resources (Emadodin *et al.*, 2019), reduction of surface and groundwater resources (Moridi, 2017), outbreak of pests and plant and animal diseases (Pourbabae *et al.*, 2014), increased migration (Khanian *et al.*, 2019), and ultimately the adverse environmental, economic, and social effects (Madani *et al.*, 2016) are among the negative effects that threaten Iran's sustainable development.

Various statistical and nonstatistical methods have been used by different researchers to understand the periodic behaviour of climatic variables in the form of different time scales. One such important method is the spectral analysis or frequency domain analysis (Rodrigo *et al.*, 2000; Yadava and Ramesh, 2007; Solgimoghaddam *et al.*, 2019). The spectrum of a time series represents the frequencies in that time series and spectral analysis is a way to identify these frequencies (Daneshmand and Mahmoudi, 2016). The history of using this method in hydroclimatological studies, especially in the field of climatology of precipitation dates back to the 1950s. One of the first studies that attempted to model the spectral behaviour of precipitations using this method were those of Scott and Shulman (1979) and Kirkyla and Hameed (1989). Some studies on the detection of precipitation harmonics by Kadioglu *et al.* (1999), Tarawneh and Kadioglu (2003), Livada *et al.* (2008), Nastos and Zerefos (2009), and Asakereh (2020). Daneshmand and Mahmoudi (2016) also showed by analysing the spectrum of time series obtained from the Effective Drought Index (EDI) for 41 stations studied in Iran which the dominant periods in the time series of droughts in Iran are very diverse and range from 2 to 22 years. In addition to these studies Asakereh (2012), Movahedi *et al.* (2012), Moghbel *et al.* (2012), Asakereh and Razmi (2012), Roradeh *et al.* (2014) for the precipitation variable, Ramzanipour *et al.* (2011) and Asakereh *et al.* (2012) for detection of apparent and latent cycles in the time series of rivers discharge and Jalili *et al.* (2011, 2013). For Lake Urmia water level time series, this method has been used a lot in Iran.

However, the use of spectral analysis in the studies related to the detection of apparent and latent droughts is very less and limited to recent decades. These studies can be divided into two categories based on a general division. The first category is the studies, which due to lack of direct access to the precipitation data, have used the drought indices, instead. Rather, they have tried to extract and analyse different periods of droughts through other variables. In this category of studies, drought and drought propensity have always been defined as a year that the precipitation was less than the long-term average (Bhalme and Mooley, 1981; Cramer, 1987; Murata, 1990; Me-Bar and Valdez, 2003; Currie, 2007; Wang *et al.*, 2007). Tree rings (Meko *et al.*, 1985), water level of rivers (Prokoph et al., 2012), surface sediments (Nelson et al., 2011), and peat (Hong et al., 2001) and agricultural productivity (Gudeta *et al.*, 2003) are some of the indicators that have been used to determine the amount of precipitation and thus understand the drought situation. In addition to these methods, determining the amount of damage caused by droughts (Jiang *et al.*, 2006), their relationship with temperature (Zhaoxia et al., 2003), and cycles of mountain fires (Garner, 2007) have been used to determine drought and thus calculate their cycles. The second category includes the studies that have directly or indirectly used various drought indicators to determine the periodicity of drought behaviour in different parts of the world. EDI (Byun *et al.*, 2008; Daneshmand and Mahmoudi, 2017), Standardized Precipitation Index (Bordi *et al.*, 2004a, 2004b; Martins *et al.*, 2012; Li *et al.*, 2013; Telesca *et al.*, 2013; Moreira *et al.*, 2015), and Palmer Drought Severity Index (PDSI) (Liu *et al.*, 2013) are among the drought indices used in this category of studies. All of these indicators, with the exception of the severity of a failure event of the Palmer Drought (PDSI) and the EDI, are defined on a monthly or seasonal time scale and will not be suitable for analysing drought propensity at longer time scales. Therefore, there is a need for an appropriate drought index that can monitor drought propensity at longer time scales.

Hashimoto *et al.* (1982) showed the effectiveness of reliability, resilience, and vulnerability (RRV)-based approach to assess the performance of water resources systems using an example of reservoir systems. Assuming that the reduction of soil moisture in a vertical soil column is similar to the performance of a water supply reservoir, the Drought Management Index (DMI) was presented using RRV based concept by Maity *et al.* (2013). Therefore, the DMI is a probabilistic drought index to describe droughts which is very different from other indicators of drought, because it considers the readiness of the system to return from drought to wet conditions, and this is a factor that has not been considered to

date in the development of management plans and reduction of damages caused by droughts. Chanda *et al.* (2014) used this index to study spatiotemporal variation drought propensity across entire Indian mainland. The results of these researchers showed that the drought propensity is low in the northern and northeastern regions of India but in the western part, the proneness is relatively high. In a global analysis, Chanda and Maity (2017) examined drought trend propensity until the end of the 21st century using DMI. They showed a significant upward trend in drought propensity in large parts of Africa, South America and Asia, and a marked downward trend in northern Europe and North America.

Since Iran is located in southwestern Asia on the desert belt of the Northern Hemisphere, most of it is dominated by subtropical high pressure cells most of the year. Therefore, most of its area is covered by areas with arid and semi-arid climates (Mahmoudi *et al.*, 2011). Therefore, considering the increasing trend of temperature (Mahmoudi *et al.*, 2019) and decreasing trend of precipitation in Iran (Mahmoudi and Rigi Chahi, 2019), the question arises whether the characteristics of droughts in Iran are changing? Therefore, the main purpose of this study is to answer this question and achieve a new methodology for the changing pattern of droughts in Iran through an analysis of their spectral patterns. Therefore, in order to achieve this goal, the long-term time series of DMI for two separate 32-year periods has been subjected to spectral analysis. Comparing the spectral changes of these two periods, the possibility of spectral changes in Iranian droughts is considered.

2 | THE STUDY AREA

Iran is part of a mountainous and highland territory called the Plateau of Iran. The area of Plateau of Iran is about 2,500,000 km^2, of which 1,648,195 km^2 belongs to Iran. This geographical area is located in Southwest Asia, between 25° and 40° north latitude and 44–64° east longitude (Ghorbani, 2013) (Figure 1).

Due to this specific geographical location and topographic features of each region of Iran, it is ruled by different climates. The average annual precipitation of Iran is about 250 mm, the spatial distribution of which is very diverse in different parts of the country. The average annual precipitation in desert areas is as low as 50 mm or less, whereas in some other places, such as the western shores of the Caspian Sea, it is around 1,800 mm (Masoodian, 2009) (Figure 2a). The spatial distribution of the average annual temperature of Iran is also a function of roughness and changes in the angle of inclination of the sun. The lowest annual temperatures in Iran

correspond to the peaks of the high mountain range and the highest is observed on the southern coast of Iran. In general, the temperature of Iran decreases from south to north and from east to west. The cooling of the air in the south–north direction is mainly due to the increase in latitude and the decrease of solar radiation, as well as the density of high mountain ranges in the north of the country. However, the decrease in temperature from east to west is due to the accumulation of the Zagros mountain range in the west of the country and the invasion of Siberian air masses into the central holes of Iran (Alijani, 1997) (Figure 2b).

In recent decades, due to the causes that are often related to global climate change, precipitation anomalies have increased in different parts of Iran and severe spatial and temporal fluctuations of drought have caused enormous damage to Iran's economy. Study conducted regarding the severity and extent of droughts in Iran during a 30 years period which ended in 2015 showed that in the years 1988, 1999, and 2007 more than 90% of Iran was dominated by drought. Besides, more than two other widespread droughts had happened in 2014 and 1998 which covered 83% and 79% of the country, respectively (Balouch, 2020).

3 | DATA AND METHODOLOGY

To study the spectral patterns of Iranian droughts based on the DMI, monthly gridded soil moisture, values (0.5 by 0.5° and in millimetres) for a period of 64 years from
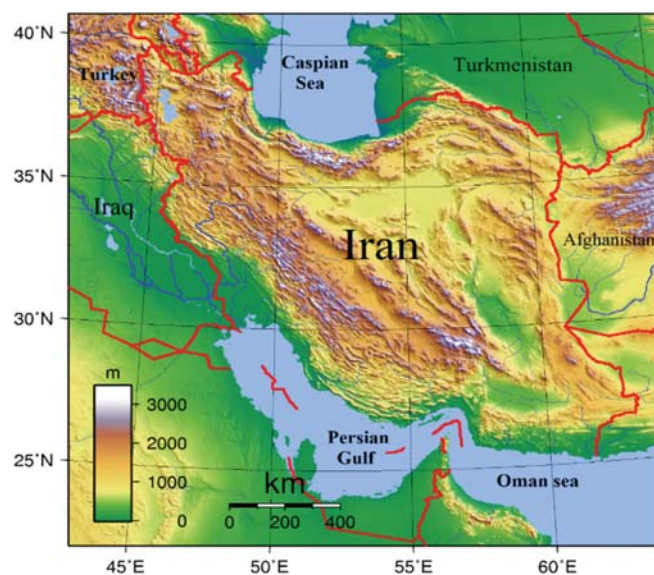

FIGURE 1 Location of Iran's political geography in Southwest Asia [Colour figure can be viewed at wileyonlinelibrary.com]
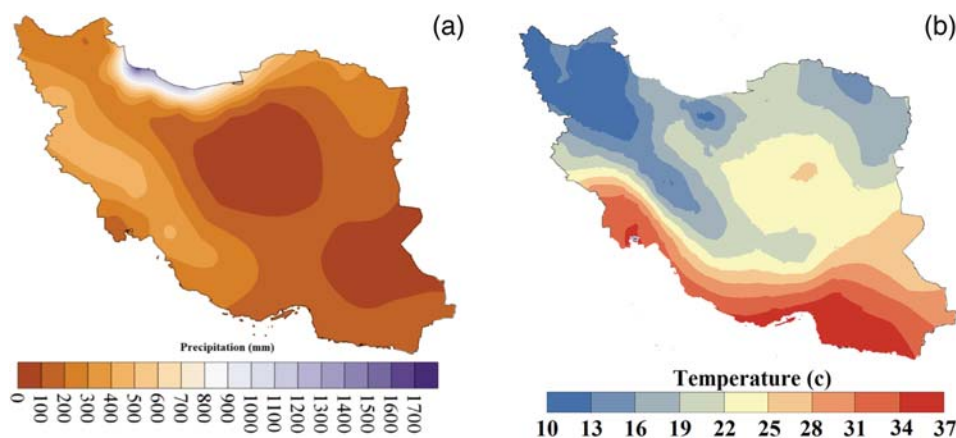
FIGURE 2 (a) Spatial distribution map of average annual precipitation of Iran, and (b) spatial distribution of the average annual temperature of Iran. Source of data for these maps is meteorological Organization of Iran [Colour figure can be viewed at wileyonlinelibrary.com]

1955 to 2018 are obtained from the Climate Prediction Center (CPC), NOAA (http://www.esrl.noaa.gov/psd/data/gridded/data.cpcsoil.html, accessed in December 2020) (Fan and van den Dool, 2004). These values are estimated based on the statements of van den Dool *et al.* (2003) using a one-layer leaky bucket model with fixed parameters in terms of space. The reason for the stability of the model parameters was their adjustment based on Oklahoma observed runoff data in the United States. In fact, this hydrological model assumes that the value of the parameters is constant for the whole world that is the water content in a single soil column to a depth of 1.6 m with a maximum water holding capacity of 760 mm and a common porosity of 0.47 (van den Dool *et al.*, 2003). It should be noted that this data is not Reanalysis data at all and it has been argued that reanalysis data are not at all reliable for this type of study due to the bias in them (van den Dool *et al.*, 2003; Fan and van den Dool, 2004). Time series of soil moisture at 622 grid points that falls within the political boarder of Iran are extracted from CPC, NOAA. The time series of this dataset are complete with no missing data. Besides, validation of the gridded data of CPC soil moisture was done by using soil moisture data obtained from 32 agricultural meteorological stations in Iran based on different statistical periods. Figure 3 shows the distribution and geographical location of the selected stations.

Determining a numerical threshold to separate dry and wet spells can be one of the major challenges in using the DMI for monitoring droughts in an area. To determine this threshold, Maity *et al.* (2013) and Chanda *et al.* (2014) proposed the use of permanent wilting point (PWP). The PWP is the minimum amount of soil moisture required for plants to prevent their wilt (Taiz and Zeiger, 1991). If soil moisture falls below this threshold, the plants can no longer leave their wilting stage and eventually die. The value of this threshold in field conditions is not a fixed value for each soil type and is determined by a combination of plant, soil and atmosphere

conditions (Rao, 1997). Specific to Iran, PWP data are not available for the whole of Iran. However, gridded data (PWP) for the entire world is developed by the Global high-resolution soil profile database for crop modelling applications, which is available at https://dataverse.harvard.edu. In this database, PWP along with 24 other soil parameters, with a spatial resolution of 10 by 10 km for each country are stored separately in *.SOL format. In this database, for each gridded point, the PWP is estimated for six layers of 5, 15, 30, 60, 100, and 200 cm above the soil surface (Han *et al.*, 2019). In this study, the weighted average of these six layers was used as the PWP threshold. The total number of gridded points extracted from this database for Iran is 15,648 gridded points. It should be noted that this database does not estimate the PWP for the desert areas of Iran, where most of the soils fall into two categories: Aridisols and Entisols with Aridic dry moisture regime (Roozitalab *et al.*, 2018). Finally, the two databases used that have different spatial distributions were also scaled. Co-scaling of the two databases is attempted such that each grid point of the soil moisture is located exactly between the four gridded points of the PWP. The average of these four points is considered as the PWP value for that gridded point of soil moisture. But for points for which the PWP was not calculated, it was decided to use a threshold value of 35% of the long-term average moisture content of that point to maintain spatial continuity. Figure 4 shows the spatial distribution of PWP values based on the Global high-resolution soil profile database for crop modelling applications within the Iranian political boundary.

3.1 | Calculation of DMI

The methodology presented in this research is broadly divided into two parts. In the first part, the steps of calculating the drought index based on soil moisture include three steps as follow:
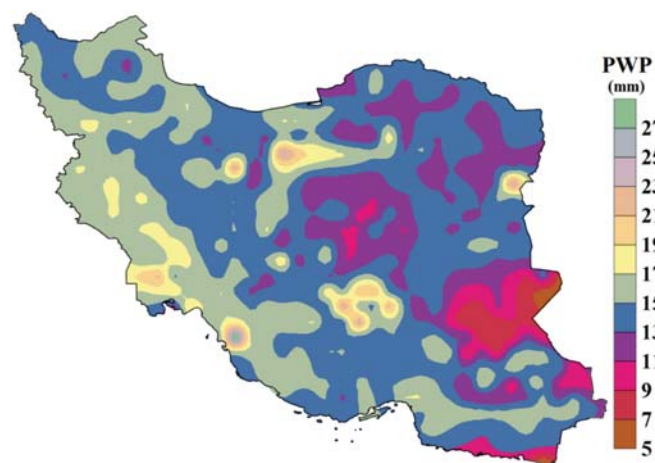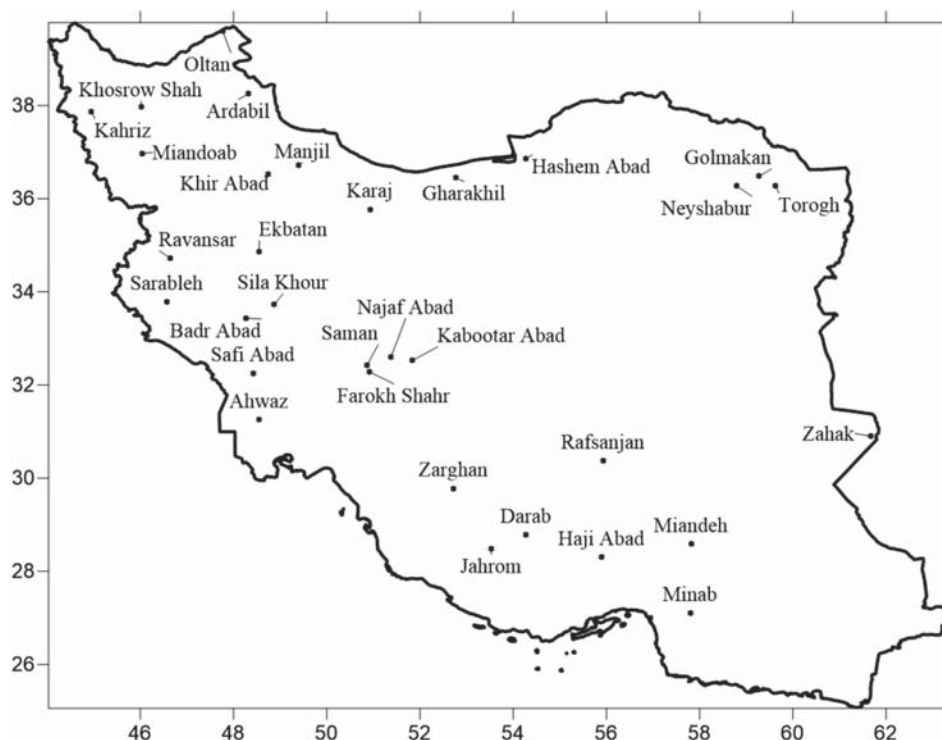
FIGURE 4 Spatial distribution of PWP values based on global
high-resolution soil profile database for crop modelling applications
for Iran's political framework (https://dataverse.harvard.edu/
dataset.xhtml?persistentId=doi:10.7910/DVN/1PEEY0) [Colour
figure can be viewed at wileyonlinelibrary.com]

1. Assessment of RRV for soil moisture time series
2. Joint probability distribution between three measures through best-fitting copula
3. Determination of DMI as a measure of the long-term characteristics of droughts

In the second part, spectral behaviour of DMI will be modelled for Iran using spectral analysis. In the following, each of these parts will be explained separately.

3.1.1 | RRV evaluation of soil moisture time series

Suppose $X_1, X_2, ..., X_n$ are time series of soil moisture with data length n to evaluate RRV. If $X_t \geq PWP$, it is considered a satisfactory stage and is indicated by the symbol S. And if $X_t < PWP$, it is recognized as an unsatisfactory stage and is marked with an F symbol.

Reliability
Reliability is defined as the probability that a system is in a satisfactory state (Hashimoto *et al.*, 1982). For soil moisture, reliability is defined as the probability that soil moisture is above the specified threshold (here PWP). Therefore, reliability α is defined as Equation (1):

$$\alpha = P(X_t \in S) \qquad (1)$$

Where S is a satisfactory stage as mentioned earlier. From time series, α is calculated as follows:

$$a = \lim_{n \to \propto} \frac{1}{n} \sum_{t=1}^{n} Z_t \qquad (2)$$

Where $Z_t = 1$, if $X_t \in S$ and $Z_t = 0$ if $X_t \in F$.

Resilience
Resilience is a measure that shows how a system can quickly return to the satisfactory stage after it has fallen

below the satisfactory threshold. This can be defined as the ratio of the probability of transition from the unsatisfactory to the satisfactory stage and also the probability of failure, that is,

$$\gamma = \frac{P(X_t \in F, X_{t+1} \in S)}{P(X_t \in F)} \tag{3}$$

where S and F are already defined. The numerator shows the ratio of the probability of transition from the unsatisfactory to the satisfactory stage, which is denoted by ρ. The number of times the system is transferred from a satisfactory stage to an unsatisfactory stage and vice versa from an unsatisfactory stage to a satisfactory stage will be equal in the long run. Finally it can be expressed as $\rho = P(X_t \in F, X_{t+1} \in S) = P(X_t \in S, X_{t+1} \in F)$. ρ can be calculated as follows

$$\rho = \underset{n \to \infty}{Lt} \frac{1}{n} \sum_{t=1}^{n} W_t \tag{4}$$

where W_t represents the event of transformation from the satisfactory to the unsatisfactory stage (or vice versa). $W_t = 1$ if $X_t \in S$, otherwise it will be $X_{t+1} \in F$ and $W_t = 0$. The denominator (3) can be expressed as $P(X_t \in F) = 1 - P(X_t \in S)$. So as explained earlier, $P(X_t \in S)$ is defined as Resilience α. Therefore, Equation (3) can also be expressed as follows:

$$\gamma = \frac{\rho}{1 - \alpha} \tag{5}$$

Vulnerability
Vulnerability measure the severity of a failure event that has already occurred. Vulnerability is defined as follows

$$v = \sum_{j \in F} s_j e_j \tag{6}$$

which s_j the numerical indicator of severity for an observation x_j which belongs to the unsatisfactory state; e_j is the probability that x_j, that is related to s_j. The most unsatisfactory and severe outcome is the result that occurred in a set of dissatisfaction situations. Regarding soil moisture, vulnerability is a probability weighted average of the soil moisture deficits (according to the PWP of the study site) of failure events. Assuming that deficits are equiprobable in terms of different magnitudes, soil moisture deficit below the PWP threshold is referred to as an indicator of severity of a failure event and

vulnerability are measured in terms of the average soil moisture deficits during failure events.

3.1.2 | Fitting a suitable copula in order to obtain joint probability distribution between three measures RRV

Interrelationships between RRV should be considered when assessing drought characteristics. To do this, the theory of copulas is used. Researchers have successfully used many copulas to perform multivariate hydrologic analysis (Maity and Kumar, 2008; Zakaria *et al.*, 2010; Maity *et al.*, 2013; Chanda *et al.*, 2014; Chanda and Maity, 2017; Das *et al.*, 2019; Poonia *et al.*, 2021; Qi *et al.*, 2021; Sahana *et al.*, 2021). Previous literature shows that negative correlations between random variables can be effectively obtained by various copulas, which will be explained in this section.

Joint probability distribution using copulas
A Copula is a function that connects univariate marginal distributions in the form of a multivariate joint distribution (Nelsen, 2006). Assume that *X* and *Y* are two continuous random variables with marginal cumulative distribution functions $F(x)$ and $G(y)$ and joint distribution function $H(x,y)$, respectively. Sklar's theorem (1959) states that for a joint distribution function *H* with margins *F* and *G* there is a copula C for all (x,y) in the extended real line $\overline{R}$, so that

$$H(x,y) = C[F(x), G(y)] \tag{7}$$

If *F* and *G* are continuous, then *C* is unique; *C* is also unique in the simultaneous range of *F* and *G*. In terms of RRV, *X* indicates reliability or resilience and *Y* indicates vulnerability, and *H* is the joint distribution. Realizing that these pairs are negatively related, seven Gumbel, Clayton, Plackett, Frank, AMH, JOE, and Gaussian copulas were selected for the most appropriate comparison to obtain the joint behaviour between reliability–vulnerability and resilience–vulnerability. Then, two goodness of fit metrics, T_n and S_n, were used to select the most suitable Coppola.

To obtain the values of the two statistics T_n and S_n, the empirical cumulative frequency function (CDF) values must first be calculated for all data points, denoting it C_n. C_n is obtained for the bivariate case as follows:

$$C_n(u) = \frac{1}{n} \sum_{i=1}^{n} I(U_{i1} \le u_1, U_{i2} \le u_2) \tag{8}$$

where $u=[u_1,u_2]$ is the reduced variables of reliability (resilience) (u_1) and vulnerability (u_2) and $I(A)=1$, if A is true and $I(A)=0$ if A is false. Reduced variables after conversion are obtained through their marginal distribution, that is, $u_2=\emptyset^{-1}(V)$ and $u_1=\emptyset^{-1}(R)$, where R is resilience, V, vulnerability and $\emptyset^{-1}$, the inverse of cumulative normal distribution. $U_{ij}(i=1,...,n\,\text{and}\,j=1,2)$ is known as pseudo-observations. These are obtained as $U_{ij}=R_{ij}/(n+1)$ where R_{ij} are the ranks of the data.

For each empirical CDF value, the CDF values are estimated using the normal (C_G), Clayton (C_C), and Gumbel (C_G) copulas for the data.

$$S_n = \int_{[0,1]^2} D_n(u)^2 dC_n(u) \tag{9}$$

$$T_n = \sup_{u \in [0,1]^2} |D_n(u)| \tag{10}$$

where $D_n(u)=\sqrt{n}(C_n-C)$ and n are the number of point data (Genest et al., 1995; Maity et al., 2013).

The results showed that the Gaussian Copula model, due to its ability to capture the Negative association between variables, is the most suitable Copula for obtaining the behaviour between reliability–vulnerability and resilience–vulnerability (more details are given in the results and discussion section). Gaussian Copula belongs to the category of elliptical copula that are able to take care of the entire range of positive and negative association between random variables. The bivariate Gaussian copula is defined as follows:

$$C_G(u,v) = \int_{-\infty}^{\varphi^{-1}(u)} \int_{-\infty}^{\varphi^{-1}(v)} \frac{1}{2\pi(1-\rho^2)^{1/2}} exp\left[-\frac{x^2-2\rho xy+y^2}{2(1-\rho^2)}\right] dy dx \tag{11}$$

The dependence parameter of this copula ρ depends on Kendall's tau, τ, which is estimated by the following equation:

$$\tau = \frac{2}{\pi} \sin^{-1}(\rho) \tag{12}$$

3.1.3 | Development of copula-based DMI as a measure of long-term characteristics of droughts

Based on the joint distribution between reliability and vulnerability, an index is developed that will convey reliability and vulnerability information simultaneously.

From the previous discussions, it became clear that more favourable conditions are shown by the increase in reliability. Here drought is recognized as an undesirable phenomenon. On the other hand, the situation becomes more unfavourable with the increase in vulnerability. Therefore, the proposed DMI should increase with increasing vulnerability and with decreasing reliability and vice versa. This can be done with a joint measure of probability that shows an exceedance of reliability and a nonexceedance of vulnerability. Therefore, DMI is defined as follows:

$$DMI = P(R>r, V \leq v) \tag{13}$$

Where $P(...)$ = probability of the event $(...)$, R = reliability, V = vulnerability and r and v = reliability and vulnerability are reduced respectively which are calculated from the time series of soil moisture using the appropriate threshold. As mentioned earlier, this threshold cannot be selected randomly. PWP is a suitable threshold based on the soil–crop composition in a particular location. To obtain the actual DMI values for a location, the PWP for that location must be used.

3.2 | Spectral analysis

After calculating the DMI for all the available gridded points inside the Iranian political borders, the stationary or nonstationary being of them was investigated by the use of the seasonal and nonseasonal differencing method, and the time series which were nonstationary became stationary by this method. In the following, the spectral analysis was used to identify the periodicity of the droughts and wet years in Iran. Various transform time series can be used for spectral analysis. Classical Fourier transform is one of the most basic and fundamental of these transformations. The classic Fourier transform is a transform from time domain to frequency domain. Using this conversion, one can accurately identify frequencies and periods. The Fourier transform states that any periodic motion can be thought of as a sum of several simple periodic motions. Fourier transform shows that a periodic function such as $f(t)$ with period p can be written as the sum of sine and cosine functions:

$$f(t) = a_0 + \sum_{n=1}^{\infty} a_n \cos(n\omega t) + \sum_{n=1}^{\infty} b_n \sin(n\omega t) \tag{14}$$

The relationship between period and frequency is as follows:

$$p = \frac{2\pi}{\omega} \tag{15}$$

Main frequency ω (first) and its multiples, $2\omega, 3\omega, ..., n\omega$ are called its harmonics. The main frequency is also called first harmonic and the frequency of each coordinate is written as an integer multiple of the main frequency or first frequency. Thus, second, third, ..., nth harmonics have frequencies $2\omega, 3\omega, ..., n\omega$, respectively. Constant a_0 displays the average value of the function. The quantities a_n and b_n represent the range of sine and cosine functions. The exact shape of a periodic function depends on the number of sine and cosine functions, as well as their range. The exact shape of the periodic function depends on the number of the range of sine and cosine functions as well as their range. In other words, the exact shape of the function determines the number of sentences selected from the series. In the mathematical representation, n, it represents the number of selected sentences from the Fourier series (Alonso and Finn, 1992).

In this research, the fast Fourier transform (FFT), the Decimation-In-Frequency FFT algorithms method has been used. FFT uses the idea of discrete Fourier transform (DFT). In fact, FFT is the fast realization of DFT that uses multiplication of matrices to reduce the computational steps (Mertins, 1999). In Figure 5, all the research stages are provided in the form of a flowchart.

4 | RESEARCH FINDINGS

4.1 | Validation of gridded data of CPC soil moisture regarding station data

Soil moisture data measured in agricultural meteorological stations in Iran have been suffering from problems such as high missing data, also the statistical period was short, and sometimes no electronic registration was done. Therefore, regarding the mentioned problems, a short 2-year period (2015–2016) was selected for all 32 agricultural meteorological stations in Iran, and their correlation coefficient was measured with the closest gridded data of CPC soil moisture. The range of values for the correlation coefficient was 0.65 in Jahrom Station, and 0.89 in Manjil Station at the probability level of $\alpha = 0.05$. Generally, it can be concluded that the correlation coefficients of stations located in arid and semi-arid regions were lower and those of stations located in wetter areas were higher. Figure 6 shows a line diagram for two time series of soil moisture in Gharakhil Station in the North of Iran. The correlation coefficient of these two time series in Gharakhil Station at the probability level of α = 0.05 was obtained at 0.7 and the time-series behaviour was almost similar to each other.

4.2 | Spatiotemporal variation of RRV

The first step in calculating the DMI is to select the appropriate moving time windows. Chanda et al. (2014) examined the sensitivity of the DMI to various time-moving windows and suggested that 5-year time-moving windows could be a good choice for calculating the DMI. Therefore, in this study, the soil moisture time series for a period of 64 years (1955–2018) were received from the CPC database, NOAA, for the framework of Iran's political borders and were divided into shorter periods of 5 years. The end result of this division was to obtain 60 blocks of 5 year moving windows (1955–1959, 1956–1960, ..., 2013–2017, 2014–2018) for the Soil moisture time series.

Then, for each of these 5-year moving windows, RRV was calculated and then their choropleth map was prepared. The total choropleth map prepared at this stage reached 180 maps. Due to the large number of maps, it was decided to sample 12 maps for each case with an interval of 5 years in the article. As can be seen in Figure 7, in most of the maps prepared for reliability, the northern parts of Iran had higher values and the southeastern parts had lower values. It should be noted that higher values indicate greater reliability and lower values indicate lower reliability. Whenever the amount of soil moisture does not fall below the set threshold even once during a period of 5 years, then the Reliability will be equal to 1 for that period, otherwise the reliability will be values lower than 1. Figure 8 shows the spatiotemporal variation of the resilience values. Resilience values also correspond exactly to reliability values and its values change between 0 and 1. As can be seen in Figure 8, large parts of the northern and western halves have high resilience and the southern and eastern halves have lower resilience. Spatiotemporal variation vulnerability (Figure 9) values also show almost identical temporal and spatial patterns with reliability and resilience. Large parts of the northern half of Iran have less vulnerability (less than 4 mm) and the southern half has more vulnerability (more than 24 mm). It should be noted that the unit for measuring vulnerability is millimetres, whereas reliability and resilience values are without units of measurement because they are measured based on probabilistic values between 1 and 0.

The reasons for the higher values of reliability and resilience and the lower values of vulnerability in the northern and western half of Iran compared to its southern and eastern half, are the existence of more precipitation, lower PWP and finally higher soil moisture. Therefore, it is unlikely that the soil moisture in these areas will remain below the PWP threshold for a long

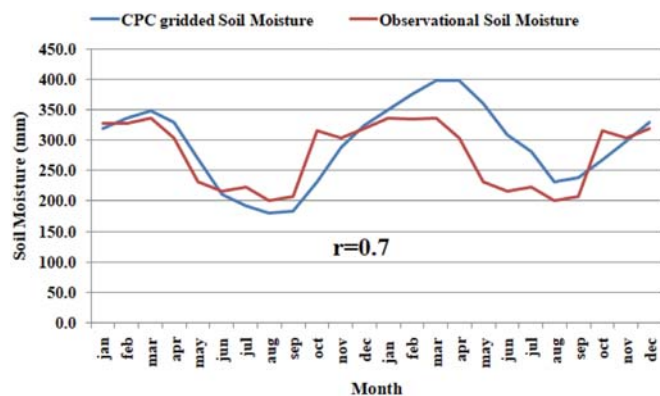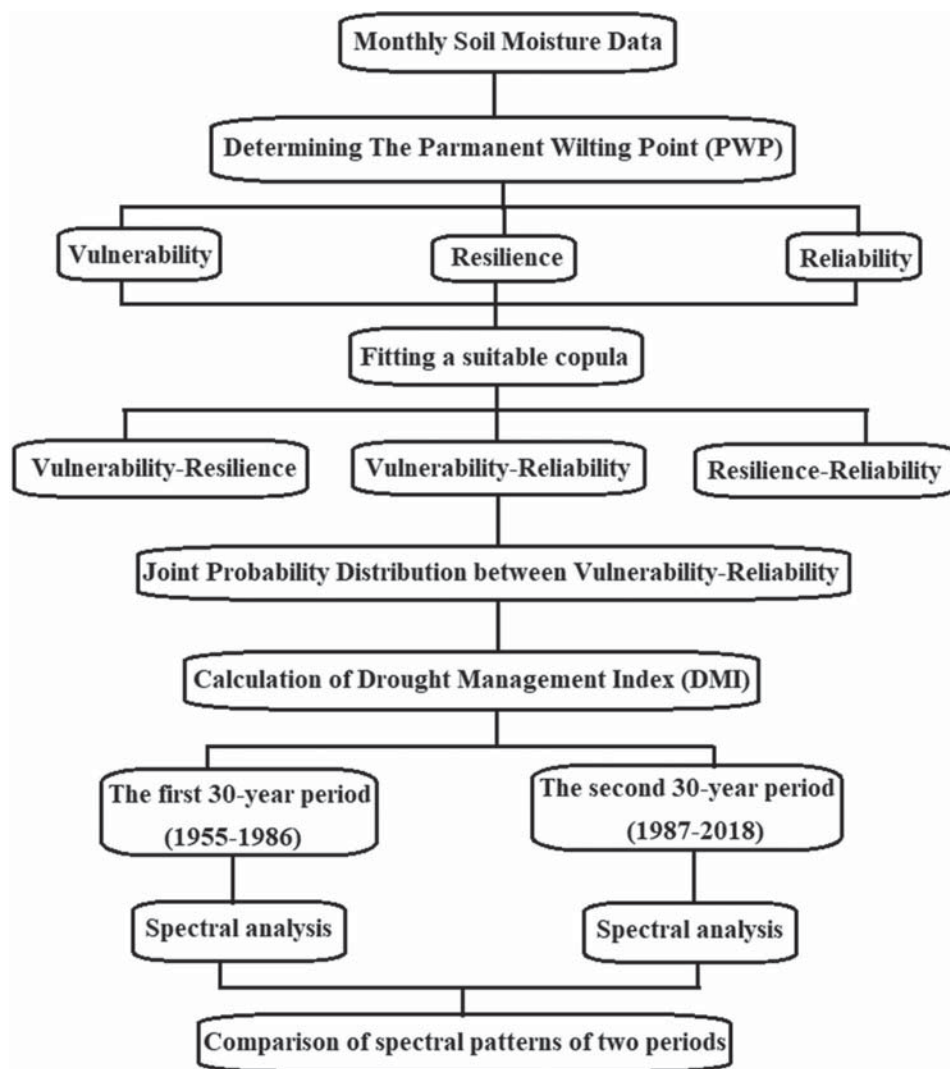FIGURE 5   The flowchart of methodology in this study

FIGURE 6   Line diagram for time series of soil moisture in Gharakhil Station in north of Iran and the time series of CPC soil moisture in the closest point to Gharakhil Station, along with the Pearson correlation coefficient value between them [Colour figure can be viewed at wileyonlinelibrary.com]
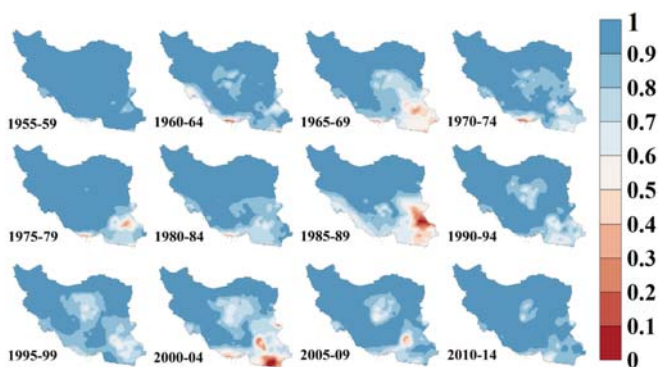

FIGURE 7   Choropleth maps of spatiotemporal variation reliability values on Iran for the period 1955–2018 (out of a total of 60 maps, for example only 12 maps with a time interval of 5 years are given) [Colour figure can be viewed at wileyonlinelibrary.com]

time. However, there is a strong tendency to stay below the PWP threshold in the southern and eastern half of Iran, due to the prevalence of arid and semi-arid climates, very low precipitation and low PWP Soil moisture. Therefore, their reliability and resilience values are very low and their vulnerability values are very high.
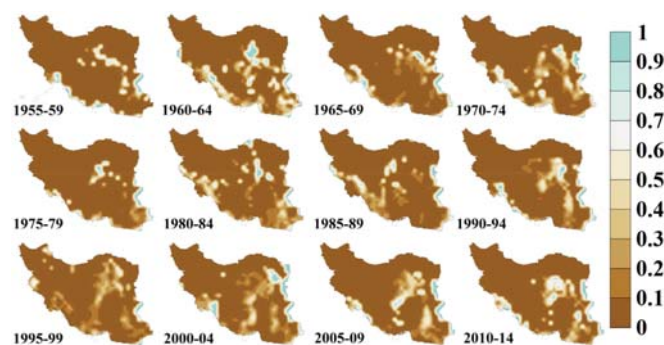
FIGURE 8 Choropleth maps of spatiotemporal variation resilience values on Iran for the period 1955–2018 (out of a total of 60 maps, for example only 12 maps with a time interval of 5 years are given) [Colour figure can be viewed at wileyonlinelibrary.com]
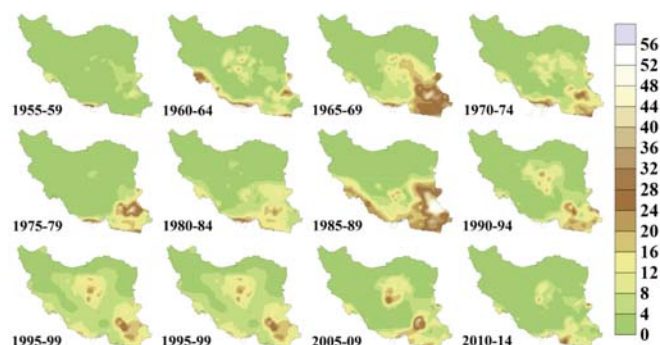

FIGURE 9 Choropleth maps of spatiotemporal variation vulnerability values on Iran for the period 1955–2018 (out of a total of 60 maps, for example only 12 maps with a time interval of 5 years are given) [Colour figure can be viewed at wileyonlinelibrary.com]

4.3 | Spatiotemporal variation of DMI

Pairwise scatter plots of RRV values for all gridded points within Iran's political borders are drawn to better understand the interrelationships between them, and Figure 10 provides an example. As shown in Figure 10, the relationship between reliability and resilience (Figure 10a) is a positive relationship and the relationship between vulnerability–resilience (Figure 10b) and vulnerability–reliability (Figure 10c) is a negative one. Kendall's tau correlation coefficient values also confirm the positive relationship between reliability and resilience (0.332) and the negative relationship between reliability and vulnerability (−0.991) and resilience and vulnerability (−0.342). Maity *et al.* (2013) and Chanda *et al.* (2014) in their studies on India also found the same relationships with slight differences in the values of RRV. Therefore, according to the joint characteristics of reliability–vulnerability and resilience–vulnerability, in this study, the combined reliability–vulnerability combination was used to develop the DMI for monitoring long-term droughts in Iran.

Then seven copulas Gumbel, Clayton, Plackett, Frank, AMH, JOE, and Normal were tried to obtain the best-fit copula for describing the joint distribution between reliability and vulnerability. As can be seen in Table 1, the statistical measure (S_n) of the Gaussian copula is much lower than that of the other joints, indicating that the Gaussian copula provides the optimum fit. However, some studies, such as Maity *et al.* (2013) and Chanda *et al.* (2014), found Plackett Copula to be a more appropriate copula for calculating the joint distribution (between resilience and vulnerability). Finally, the Gaussian copula was

selected to obtain the joint distribution between reliability and vulnerability in this study. Therefore, according to this index, drought is an unfavourable climatic phenomenon that is associated with increased vulnerability and decreased reliability in an area.

Spatial variations of DMI were also examined by a set of 60 maps prepared for the entire study period (1955–2018). Out of these 60 maps, 12 maps are given as an example in Figure 10 with an interval of 5 years. As can be seen in Figure 11, the values of the DMI are always and consistently high for the south, east and centre of Iran, which shows the great tendency of these regions to drought, while for the western and northern half of Iran, this index shows a much lower value. These variations in the values of DMI in the geographical area of Iran can have different causes, but certainly spatial extent, climatic diversity, topography, soil type, and temporal–spatial distribution of precipitation have played the most important role.

To study the DMI temporal variations, out of a total of 622 gridded points within Iran's political borders, eight sample points were selected and their time series diagrams were prepared (Figure 12). The selection of these eight points was based on the highest value of the DMI measured during the study period. For example, point 'a' represents the point where the highest DMI was between 0.6 and 0.7. Point 'b' represents the point where the highest DMI was between 0.5 and 0.6. Finally, point 'h' refers to a point where DMI values are zero for the entire period under study. According to these graphs (Figure 12a–h) it can be clearly seen that in all of them, with the exception of graph h, where all the DMI values were zero, it is an almost periodic definite behaviour is observed in them.
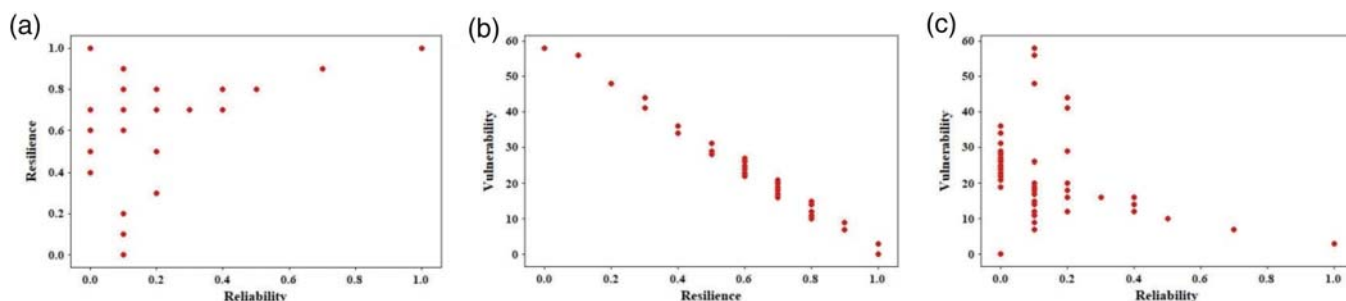
FIGURE 10 Pairwise scatter plot between (a) reliability-resilience, (b) resilience–vulnerability and (c) reliability–vulnerability [Colour figure can be viewed at wileyonlinelibrary.com]

TABLE 1 Fitting copulas given to pairs of resilience and vulnerability variables to obtain a joint probability distribution

Copula	Gumbel	Clayton	Plackett	Frank	AMH	JOE	Normal
S_n	0.3696	0.24538	0.5631	0.8452	1.2485	1.1113	0.10608

FIGURE 11 Choropleth maps of spatiotemporal variation DMI values on Iran for the period 1955–2018 (out of a total of 60 maps, for example only 12 maps with a time interval of 5 years are given) [Colour figure can be viewed at wileyonlinelibrary.com]
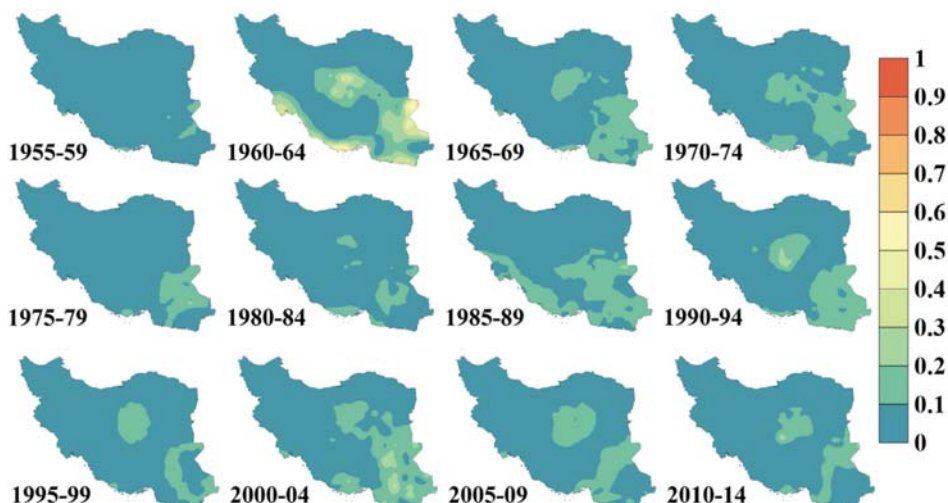
4.4 | Spectral analysis of DMI time series

To study the changing spectral Pattern of droughts in Iran, first the Soil moisture time series that were received for a period of 64 years (1955–2018) from the CPC database, NOAA, was divided into two equal periods of 32 years. Then the DMI was calculated based on 5 year moving windows for both periods separately. Spectral analysis by Fourier transform method was used to identify the dominant periods or frequencies in the DMI time series. Given that Fourier transform is problematic in the nonstationary series Spectral analysis, the stationary condition of the DMI series for both periods was examined for all gridded points within Iran's political borders. In places where there was no static condition, static transformations were performed using seasonal and non-seasonal differencing. Then the data were analysed spectrally.

The output of Spectral analysis on the DMI time series is a periodogram (Figure 13). This periodogram actually shows the relationship between power and frequency. The high power at a frequency indicates the predominance of that frequency during the desired time series. In this study, frequency is shown in terms of Cycle per year. In other words, periodicities or cycles are measured on a yearly basis. For example, the periodograms of a selected point (point a in Figure 12) are shown separately for the first 32-year period (1986–1955) and the second 30-year period (1987–2018) in Figure 13. Based on these periodograms, it can be seen that in the first 30 years, the three dominant Periodicities based on the highest powers were Periodicities of 2.73, 2.5, and 2.14 years, respectively (Figure 13a), while in the second 32-year period, these periodicities changed in nature and the three dominant periodicities of this period were cycles of 10, 3.75, and 2 years, respectively (Figure 13b).
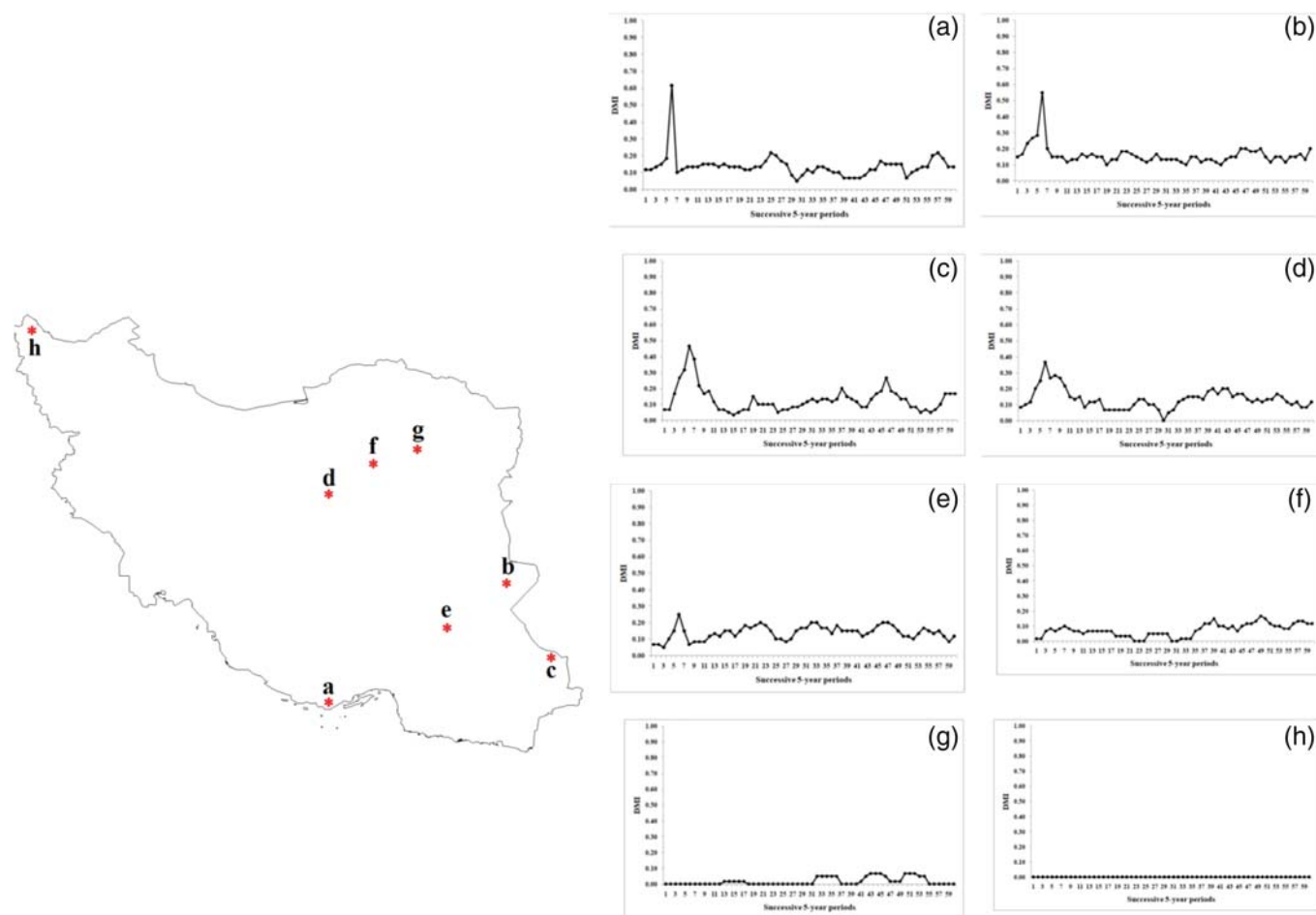
FIGURE 12 DMI time series changes plot for 8 selected points during the period 1955–2018. The horizontal axis numbers from number 1 represent the time period 1959–1955, number 2 represents the time period 1960–1956, ... and number 60 represents the time period 2018–2014 [Colour figure can be viewed at wileyonlinelibrary.com]
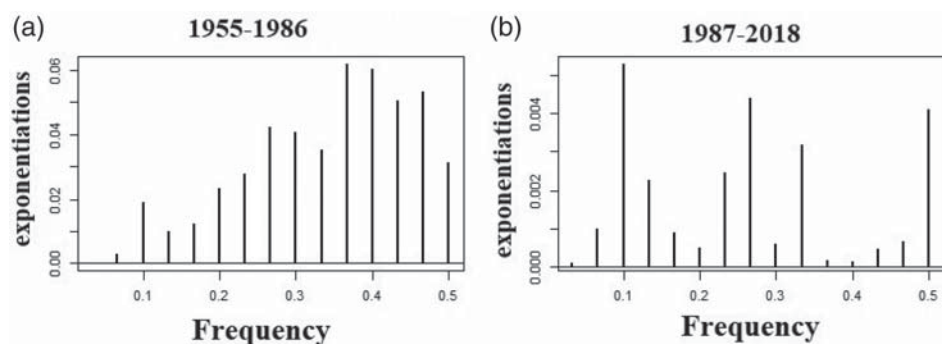

FIGURE 13 Periodograms of a selected point (point a in Figure 9) separately for (a) the first 32-year period (1986–1995) and (b) the second 32-year period (1987–2018)

Accordingly, for all gridded points within Iran's political borders, the three periodicities or the first three periodic components with the highest powers were extracted for both the first 32-year period (1955–1986) and the second 32-year period (1987–2018). In Figure 14, the left panel shows the spatial distribution of the three Periodicities or the first three periodic components of the first 32-year period (1955–1986) and the right panel shows the

spatial distribution of the three periodicities or the first three periodic components of the second 32-year period (1987–2018). As can be seen in Figure 14, the dominant periods in the DMI time series are very diverse and include periods of 2 to 30 years. Since the value of DMI for parts of north, northwest, northeast, and west of Iran in all two periods studied has always been zero, no change should be expected for these parts of Iran.

Comparing the maps of these two periods for the south, southwest, southeast, east, and centre of Iran, these differences are clearly visible (Figure 14).

Finally, in order to obtain a better view of the spectral changes between the two periods studied, a map of their changes in periodicities was prepared. In Figure 15, the points whose periodicities have changed in nature from shorter periodicities in the first 32 years to longer periodicities in the second 32 years are shown as red circles. However, periodicities that were longer in the first 32-year period and shortened in the second 32-year period are shown as green dots. According to Figure 15, it is clear that for parts of the northwest, northeast, west, southwest, and south of Iran, periodicity of droughts

have been prolonged whereas the periodicity of droughts in the eastern, southeastern and central parts of Iran has been shortened. The results of this study are almost in line with the results of Mahmoudi and Daneshmand (2018). By spectral analysis of time series obtained from EDI for 41 stations studied in Iran, they showed that the dominant periods in the drought time series of Iran are very diverse and range from 2 to 22 years. They also claim that the severity of wet years was declining in Iran and the severity of drought was increasing. In addition, Mahmoudi and Daneshmand (2018) have reported that the probability of droughts in Iran is increasing and their return period is shorter than the past.
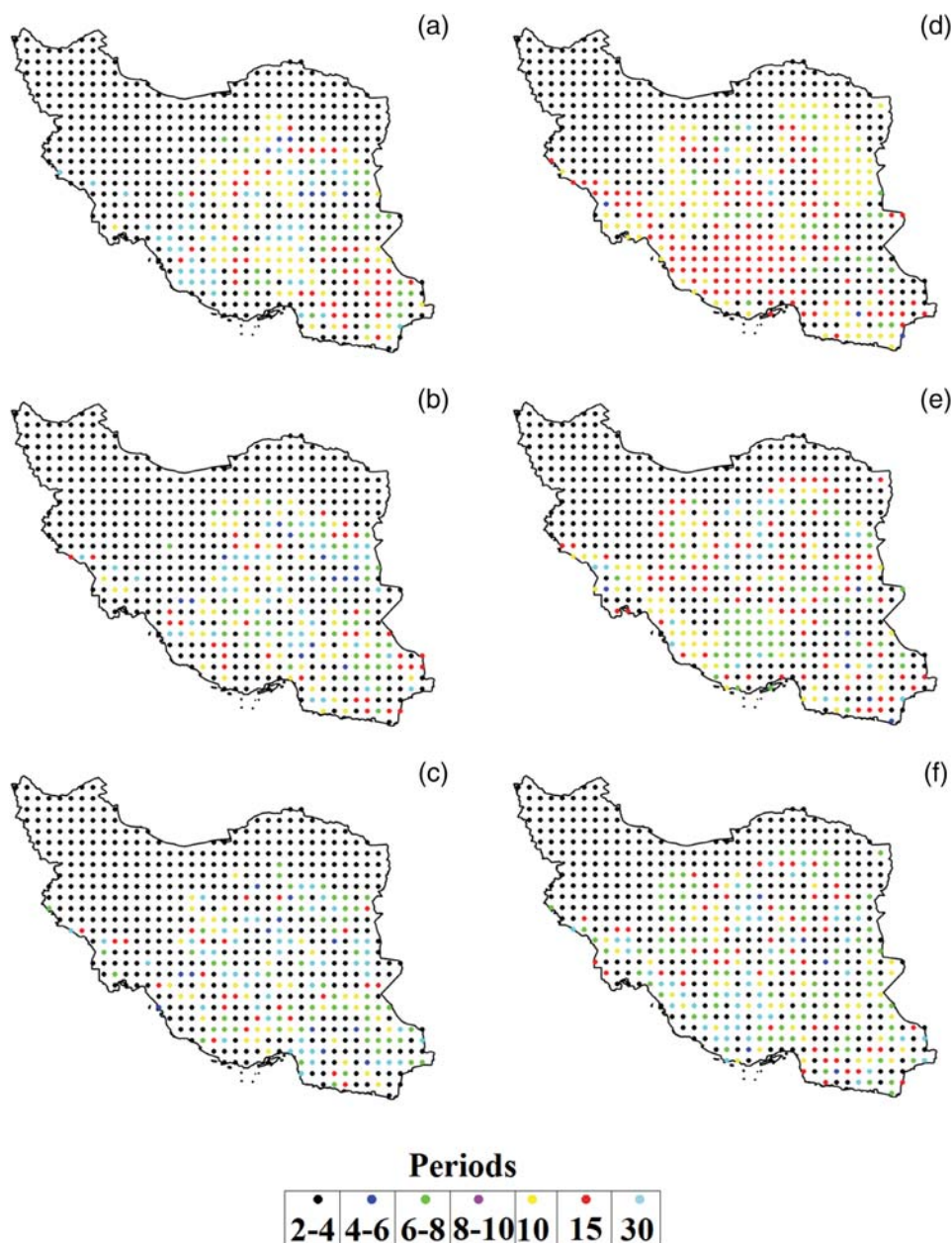

FIGURE 14 The first three periodicities with the highest powers for the first 32-year period (1955–1986) and the second 32-year period (1987–2018) [Colour figure can be viewed at wileyonlinelibrary.com]
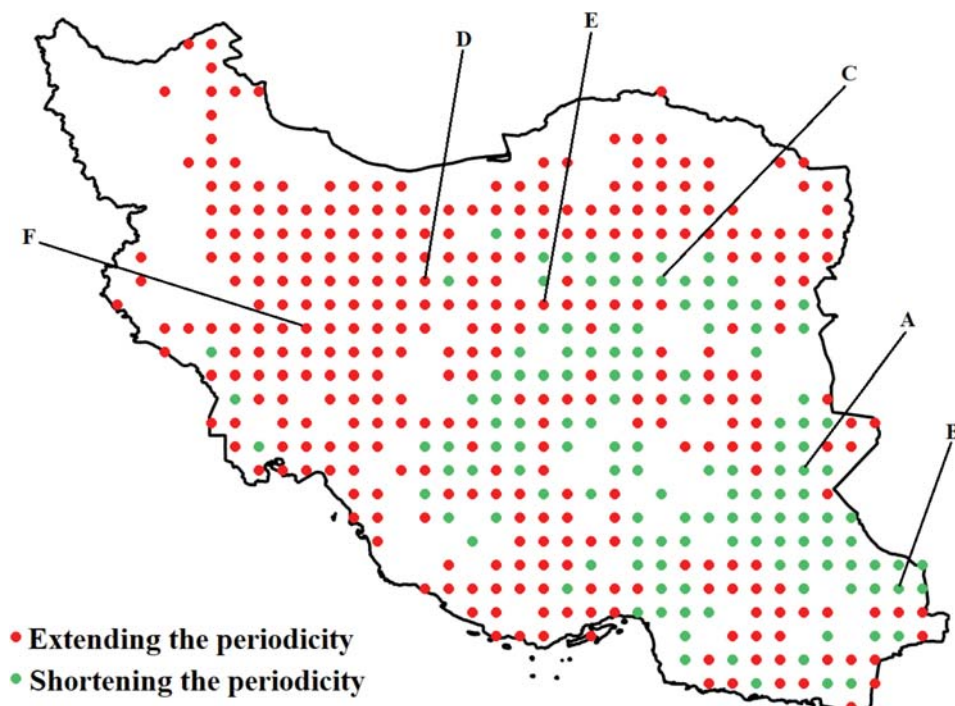
Periods

•	•	•	•	•	•	•
2-4	4-6	6-8	8-10	10	15	30

TABLE 2 The droughts' spectral patterns changes in the select points from the first 32-year to the second 32-year period

Points	The first 32-year period (1955–1986)			The second 32-year period (1987–2018)		
	First periodicity	Second periodicity	Third periodicity	First periodicity	Second periodicity	Third periodicity
A	3.33	7.50	15	3.33	2.14	6
B	7.50	15	3.75	3.33	2.14	3
C	15	30	3.75	7.5	3	15
D	2.73	10	2.14	15	2.14	3.75
E	10	2.31	3.75	3	10	30
F	3.33	7.50	3.75	10	15	7.5

Note: The points A, B, and C represent the points with shorter periodicity in the first 32-year period than the second 32-year period (marked with a darker colour), and the points D, E, and F are those whose periodicity have been longer in the first 32-year period than the second 32-year period.

In Tables 2, 6 points out of 622 gridded points whose droughts spectral patterns have been changed over time, within the Iranian political borders, were chosen as samples. The geographical location of these 6 points has been marked by capital letters (A–F) in Figure 12. These six points selection method was that points A, B, and C represent points whose periodicity has been shortened from the first 32-year period to the second 32-year period. The points D, E, and F are those whose periodicity has been longer in the first 32-year period than the second 32-year period. Based on Table 2, these changes in the spectral patterns of Iran's droughts can be clearly seen in their periodicity.

5 | CONCLUSION

The main objective of the current study was to investigate the changes in spectral patterns of droughts in Iran. To achieve this goal, first, the long-term time series of DMI was calculated based on components such as vulnerability, reliability, and resilience, for 60 years by the use of gridded soil moisture data from the CPC NOAA, within the Iranian political borders. The results indicated that the DMI's value for the southern, eastern, and central areas of Iran has been continuously high, while it has been low for the western and northern halves. The high and low values of this index are indicative of very high

and very low propensity for drought in these areas, respectively. These differences in DMI values in the Iranian geographical area can be due to different reasons such as the spatial extent, climatic diversity, topography, soil type, and temporal–spatial distribution of precipitation.

For extraction of the spectral patterns of the droughts in Iran during the 60 years under investigation (1958–2018), it was divided into two 32-year periods. Then, by the use of the spectral analysis, the three first periodicities or periodic components with the highest power were extracted for each period and ultimately, these periodicities were compared. The results indicated that the drought periodicities in the north-west, north-east, west, south-west, and south of Iran have become longer, that is, their nature has been changed from shorter periodicities to longer ones. This change of nature in their first three periodicities has been sometimes from 2–10 years to 2–15 years, from 2–10 years to 3–30 years, and from 3–8 years to 8–15 years. However, the periodicities of droughts in the eastern, south-eastern, and central Iran has changed from longer periodicities to shorter ones. It has been changed from 3–15 years to 2–6 years, from 3–15 years to 2–3 years, and from 3–30 years to 3–15 years. In a more general conclusion, it can be stated that the return periods in the northeastern, northwestern, western, southwestern, and southern parts of Iran have become longer, while it has become shorter in the east, southeast, and centre. These changes led to the increase in the frequency of droughts in the east, southeast, and centre, making them among the most vulnerable areas in terms of droughts. Thus, regarding the revealing changes in the spectral patterns of droughts in Iran, water resources management policy-making must be revised based on these changes, especially in the arid and semi-arid areas, so that its adverse effects on the farmers' sustainable livelihood would be reduced.

However, apart from the results of this study, there would be remained two basic questions that should be responded to in further studies. First question: the long-term process of the propensity to droughts in Iran is based on what spatial–temporal patterns? Are these spatial–temporal patterns in line with the results obtained from the current study? The second question: are the spectral patterns of other drought indices, especially the meteorological drought indices, in line with the results of the current study which has been focused on the long-term drought propensity?

AUTHOR CONTRIBUTIONS

Peyman Mahmoudi: Conceptualization; data curation; formal analysis; investigation; methodology; project administration; resources; supervision; validation. **Rajib Maity:** Conceptualization; data curation; formal analysis; investigation; methodology; project administration; resources; supervision; validation. **Seyed Mahdi Amir Jahanshahi:** Data curation; formal analysis; investigation; methodology; software; validation. **Kironmala Chanda:** Conceptualization; investigation; methodology.

ORCID

Peyman Mahmoudi https://orcid.org/0000-0003-2138-0973
Rajib Maity https://orcid.org/0000-0001-5631-9553
Seyed Mahdi Amir Jahanshahi https://orcid.org/0000-0002-3571-886X
Kironmala Chanda https://orcid.org/0000-0001-5874-107X

REFERENCES

Alijani, B. (1997). *Climate of Iran*. Tehran, Iran: Payam Noor University Press. (In Persian).

Alonso, M. and Finn, E.J. (1992) *Physics*, 2nd edition. Reading, MA: Addison-Wesley.

Asakereh, H. (2012) Frequency distribution change of extreme precipitation in Zanjan City. *Geography and Environment Planning Journal*, 45(1), 51–66 (In Persian).

Asakereh, H. (2020) Decadal variation in precipitation regime in northwest of Iran. *Theoretical and Applied Climatology*, 139, 461–471.

Asakereh, H. and Razmi, R. (2012) Analysis of annual precipitation changes in northwest of Iran. *Geography and Environment Planning Journal*, 47(3), 147–164 (In Persian).

Asakereh, H., Khoshraftar, R. and Sotudeh, F. (2012) Cycles analysis of time discharge and rainfall series of Mashinekhaneh Station (Garakanrood of Talesh catchment). *Water and Soil*, 26(5), 1128–1139 (In Persian).

Balouch, P. (2020) *Analyzing Iran's Local and Regional Droughts Using the Theory of Runs and Standardized Precipitation Index (SPI)*. M.Sc. thesis. Zahedan, Iran: University of Sistan and Baluchestan.

Bhalme, H.N. and Mooley, D.A. (1981) Cyclic fluctuations in the flood area and relationship with the double (hale) sunspot cycle. *Journal of Applied Meteorology*, 20, 1041–1048.

Bordi, I., Fraedrich, K., Gerstengarbe, F.-W., Werner, P.C. and Sutera, A. (2004a) Potential predictability of dry and wet periods: Sicily and Elbe-Basin (Germany). *Theoretical and Applied Climatology*, 77, 125–138.

Bordi, I., Fraedrich, K., Jiang, J.M. and Sutera, A. (2004b) Spatio-temporal variability of dry and wet periods in eastern China. *Theoretical and Applied Climatology*, 79, 81–91.

Byun, H.R., Lee, S.J., Morid, S., Choi, K.S., Lee, S.M. and Kim, D. W. (2008) A study on the periodicities of droughts in Korea. *Asia-Pacific Journal of Atmospheric Sciences*, 44, 417–441.

Chanda, K. and Maity, R. (2017) Assessment of trend in global drought propensity in the twenty-first century using Drought Management Index. *Water Resources Management*, 31, 1209–1225.

Chanda, K., Maity, R., Sharma, A. and Mehrotra, R. (2014) Spatio-temporal variation of long-term drought propensity through reliability-resilience-vulnerability based Drought Management Index. *Water Resources Research*, 50, 7662–7676.

Cramer, J.S. (1987) Mean and variance of R2 in small and moderate samples. *Journal of Econometrics*, 35, 253–266.

Currie, R.G. (2007) Luni-solar 18.6- and solar cycle 10–11-year signals in Chinese dryness-wetness indices. *International Journal of Climatology*, 15, 497–515.

Daneshmand, H. and Mahmoudi, P. (2016) A spectral analysis of Iran's droughts. *Iranian Journal of Geophysics*, 5(1), 28–47 (In Persian).

Daneshmand, H. and Mahmoudi, P. (2017) Estimation and assessment of temporal stability of periodicities of droughts in Iran. *Water Resources Management*, 31, 3413–3426.

Das, J., Jha, S. and Goyal, M.K. (2019) Non-stationary and copula-based approach to assess the drought characteristics encompassing climate indices over the Himalayan states in India. *Journal of Hydrology*, 580, 124356.

Emadodin, I., Reinsch, T. and Taube, F. (2019) Drought and desertification in Iran. *Hydrology*, 6(3), 1–12.

Fan, Y. and van den Dool, H. (2004) Climate prediction center global monthly soil moisture data set at 0.5 degree resolution for 1948 to present. *Journal of Geophysical Research*, 109(10), D10102.

Garner, M.E. (2007) *Risk Mitigation of Wildfire Hazards at the Wild and Urban Interface of Northwest Arkansas*. Fayetteville, AR: Center for Advanced Spatial Technologies (CAST), University of Arkansas. http://www.cast.uark.edu/student_pubs/mike_gar-ner/chapter5.html.

Genest, C., Ghoudi, K. and Rivest, L.P. (1995) A semiparametric estimation procedure of dependence parameter in multivariate families of distributions. *Biometrika*, 82(3), 543–552.

Ghorbani, M. (2013) *The Economic Geology of Iran: Mineral Deposits and Natural Resources*. Dordrecht: Springer.

Gudeta, Z., Oosthuizen, L.K. and van Schalkwyk, H.D. (2003) Extracting a cycle from Ethiopian agricultural gross domestic product (GDP). *Eastern Africa Social Science Research Review*, 19, 111–120.

Han, E., Amor, V.M., Ines, A.V.M. and Koo, J. (2019) Development of a 10-km resolution global soil profile dataset for crop modeling applications. *Environmental Modelling & Software*, 119, 70–83.

Hashimoto, T., Stedinger, J.R. and Loucks, D.P. (1982) Reliability, resiliency, and vulnerability criteria for water resource system performance evaluation. *Water Resources Research*, 18(1), 14–20.

Hong, Y.T., Wang, Z.G., Jiang, H.B., Lin, Q.H., Hong, B., Zhu, Y.X., Wang, Y., Xu, L.S., Leng, X.T. and Li, H.D. (2001) A 6000-year record of changes in drought and precipitation in northeastern China based on a δ13C time series from peat cellulose. *Earth and Planetary Science Letters*, 185(1-2), 111–119.

Jalili, S., Morid, S., Banakar, A. and Namdar Ghanbari, R. (2011) Assessing the effect of SOI and NAO indices on Lake Urmia water level variations, application of spectral analysis. *Water and Soil*, 25(1), 140–149 (In Persian).

Jalili, S., Morid, S., Banakar, A. and Namdar Ghanbari, R. (2013) Spectral analysis of periodic behavior of Lake Urmia water level time series. *Water and Soil Conservation*, 19(4), 25–46 (In Persian).

Jiang, T., Q. Zhang, Q., Zhu, D. M., Wu, Y. J., 2006. Yangtze floods and droughts (China) and teleconnections with ENSO activities (1470–2003). *Quaternary International*, 144, 29–37.

Joneidi, H., Azizi, N., Osati, K. and Bandak, I. (2020) The effects of precipitation variability on the canopy cover of forage species in arid rangelands, Iran. *Arabian Journal of Geosciences*, 13(18), 1–9.

Kaboli, S., Hekmatzadeh, A.A., Darabi, H. and Haghighi, A.T. (2021) Variation in physical characteristics of rainfall in Iran, determined using daily rainfall concentration index and monthly rainfall percentage index. *Theoretical and Applied Climatology*, 144, 507–520.

Kadioglu, M., Ozturk, N., Erdun, H. and Sen, Z. (1999) On the precipitation climatology of Turkey by harmonic analysis. *International Journal of Climatology*, 19, 1717–1728.

Khanian, M., Serpoush, B. and Gheitarani, N. (2019) Balance between place attachment and migration based on subjective adaptive capacity in response to climate change: the case of Famenin County in Western Iran. *Climate and Development*, 11(1), 69–82.

Kirkyla, K.I. and Hameed, S. (1989) Harmonic analysis of the seasonal cycle in precipitation over the United States: a comparison between observations and a general circulation model. *Journal of Climate*, 2(12), 1463–1475.

Li, B., Su, H., Chen, F., Li, S., Tian, S., Qin, Y, Zhang, R., Chen, S., Yang, Y. and Rong, Y. (2013) The changing pattern of droughts in the Lancang River Basin during 1960–2005. *Theoretical and Applied Climatology*, 111, 401–415.

Livada, I., Charalambous, G. and Assimakopoulos, M.N. (2008) Spatial and temporal study of precipitation characteristics over Greece. *Theoretical and Applied Climatology*, 93, 45–55.

Liu, Z., Zhou, P., Zhang, F., Liu, X. and Chen, G. (2013) Spatiotemporal characteristics of dryness/wetness conditions across Qinghai Province, Northwest China. *Agricultural and Forest Meteorology*, 182, 101–108.

Madani, K., AghaKouchak, A. and Mirchi, A. (2016) Iran's socio-economic drought: challenges of a water-bankrupt nation. *Iranian Studies*, 49(6), 997–1016.

Mahmoudi, P. and Daneshmand, H. (2018) The application of wavelet analysis to identify the periodic behavior of droughts in Iran. *Journal of Geography and Environmental Hazards*, 7(25), 153–168 (In Persian).

Mahmoudi, P., Rigi Chahi, A., 2019. *Climate Change Impact on Spatial and Temporal Distribution of Precipitation in Iran*. 6th International Regional Conference of Climate Change, November 18–19, Tehran, Iran.

Mahmoudi, P., Kalim, D. M., Amirmoradi, M. R., 2011. *Investigation of Iran Vulnerability Trend to Desertification with Approach of Climate Change*. International Conference on Environmental Science and Development—ICESD, January 7–9, Mumbai, India.

Mahmoudi, P., Mohammadi, M. and Daneshmand, H. (2019) Investigating the trend of average changes of annual temperatures in Iran. *International Journal of Environmental Science and Technology*, 16, 1079–1092.

Maity, R. and Kumar, N.D. (2008) Probabilistic prediction of hydroclimatic variables with nonparametric quantification of uncertainty. *Journal of Geophysical Research*, 113(D14), D14105.

Maity, R., Sharma, A., Nagesh Kumar, D. and Chanda, K. (2013) Characterizing drought using the reliability-resilience-vulnerability concept. *Journal of Hydrologic Engineering*, 18(7), 859–869.

Masoodian, A. (2009) *Iran's Weather*, 1st edition. Mashhad: Sharia Toos, In Persian.

Mertins, A. (1999) *Signal Analysis: Wavelets, Filter Banks, Time-Frequency Transformation and Applications*. New York: Wiley.

Martins, D.S., Raziei, T., Paulo, A.A. and Pereira, L.S. (2012) Spatial and temporal variability of precipitation and drought in Portugal. *Natural Hazards and Earth System Sciences*, 12, 1493–1501.

Me-Bar, Y. and Valdez, F. (2003) Droughts as random events in the Maya lowlands. *Journal of Archaeological Science*, 30, 1599–1606.

Meko, D.M., Stockton, C.W. and Blasing, T.J. (1985) Periodicity in tree rings from the corn belt. *Science*, 229, 381–384.

Moghbel, M., Davoudi, M., Neyestanim, A. and Taghavi, F. (2012) Identifying the changes in precipitation regime over Iran during recent decades. *Nivar*, 72, 55–65 (In Persian).

Moreira, E.E., Martins, D.S. and Pereira, L.S. (2015) Assessing drought cycles in SPI time series using a Fourier analysis. *Natural Hazards and Earth System Sciences*, 15, 571–585.

Moridi, A. (2017) State of water resources in Iran. *International Journal of Hydrogen Energy*, 1(4), 111–114.

Movahedi, S., Asakereh, H., Sabziparvar, A.A., Masoodian, S.A. and Maryanaji, Z. (2012) Assessment of variability of precipitation regime in Iran. *Journal of Water and Soil*, 25(6), 1434–1447 (In Persian).

Murata, A. (1990) Regionality and periodicity observed in rainfall variations of the Baiu season over Japan. *International Journal of Climatology*, 10, 627–646.

Nastos, P.T. and Zerefos, C.S. (2009) Cyclic modes of the intra-annual variability of precipitation in Greece. *Advances in Geosciences*, 25, 45–50.

Nelsen, R.B. (2006) *An Introduction to Copulas*. New York: Springer.

Nelson, D.B., Abbott, M.B., Steinman, B., Polissar, P.J., Stansell, N. D., Ortiz, J.D., Rosenmeier, M.F., Finney, B.P. and Riedel, J. (2011) Drought variability in the Pacific Northwest from a 6,000-yr lake sediment record. *Proceedings of the National Academy of Sciences*, 108(10), 3870–3875.

Poonia, V., Srinidha, J. and Goyel, M.K. (2021) Copula based analysis of meteorological, hydrological and agricultural drought characteristics across Indian river basins. *International Journal of Climatology*, 41(9), 4637–4652.

Prokoph, A., Adamowski, J. and Adamowski, K. (2012) Influence of the 11 year solar cycle on annual streamflow maxima in Southern Canada. *Journal of Hydrology*, 442-443, 55–62.

Pourbabae, H., Rahimi, V. and Adel, M.N. (2014) Effects of drought on plant species diversity and productivity in the oak forests of Western Iran. *Ecologia Balkanica*, 6(1), 61–71.

Qi, W., Feng, L., Yang, H., Zhu, X., Liu, Y. and Liu, J. (2021) Weakening flood, intensifying hydrological drought severity and decreasing drought probability in Northeast China. *Journal of Hydrology: Regional Studies*, 30, 100941.

Ramzanipour, M., Roshani, M. and Sotodeh, F. (2011) An analysis of the variation, trend, and cycles of precipitation and discharge in the west og Guilan provinve (case study: Navroud basin). *Journal of Studies of Human Settlements Planning*, 5(13), 60–79 (In Persian).

Rao, N.H. (1997) Grouping water storage properties of Indian soils for soil water balance model applications. *Agricultural Water Management*, 36, 99–109.

Rodrigo, F.S., Esteban-Parra, M.J., Pozo-Vazques, D. and CastroDiez, Y. (2000) Rainfall variability in southern Spain on decadal to centennial time scales. *International Journal of Climatology*, 20, 721–732.

Roozitalab, M.H., Siadat, H. and Farshad, A. (2018) *The Soils of Iran*. Dordrecht: Springer.

Roradeh, H., Yousefi, Y., Masoompour Samakosh, J. and Feizi, V. (2014) Temporal and spatial analysis of extreme precipitation characteristics in Iran. *Geography and Environment Planning Journal*, 25(2), 25–36 (In Persian).

Sahana, V., Sreekumar, P., Mondal, A. and Rajsekhar, D. (2021) On the rarity of the 2015 drought in India: a country-wide drought atlas using the multivariate standardized drought index and copula-based severity-duration-frequency curves. *Journal of Hydrology: Regional Studies*, 30, 100727.

Scott, C.M. and Shulman, M.D. (1979) An areal and temporal analysis of precipitation in the northeastern United States. *Journal of Applied Meteorology*, 18(5), 627–633.

Shean, M. (2008) *Iran: 2008/09 Wheat Production Declines Due to Drought*. United States Department of Agriculture, Foreign Agricultural Service. https://ipad.fas.usda.gov/s/2008/05/Iran_may2008.htm (Accessed 9 May 2008).

Solgimoghaddam, M., Khosravi, Y., Asakereh, H. and Doostkamian, M. (2019) The validation of the thermal regions in Iran with an emphasis on the identification of the climatic cycles. *Journal of Human Environment and Health Promotion*, 5(1), 1–8.

Taiz, L. and Zeiger, E. (1991) *Plant Physiology*. Redwood City, CA: Benjamin/Cummings.

Tarawneh, Q. and Kadioglu, M. (2003) An analysis of precipitation climatology in Jordan. *Theoretical and Applied Climatology*, 74, 123–136.

Telesca, L., Vicente-Serrano, S.M. and López-Moreno, J.I. (2013) Power spectral characteristics of drought indices in the Ebro river basin at different temporal scales. *Stochastic Environmental Research and Risk Assessment*, 27, 1155–1170.

Vaghefi, S.A., Keykhai, M., Jahanbakhshi, F., Sheikholeslami, J., Ahmadi, A., Yang, H. and Abbaspour, K.C. (2019) The future of extreme climate in Iran. *Scientific Reports*, 9, 1464.

van den Dool, H., Huang, J. and Fan, Y. (2003) Performance and analysis of the constructed analogue method applied to US soil moisture applied over 1981–2001. *Journal of Geophysical Research*, 108, 1–16.

Wang, B., Jhun, J.G. and Moon, B.K. (2007) Variability and singularity of Seoul, South Korea, Rainy Season (1778–2004). *Journal of Climate*, 20, 2572–2580.

Yadava, M.G. & Ramesh, R. (2007) Significant longer-term periodicities in the proxy record of the Indian monsoon rainfall. *New Astronomy*, 12(7), 544–555.

Zakaria, R., Metcalfe, A., Piantadosi, J., Boland, J. and Howlett, P. (2010) Using the skew-t copula to model bivariate rainfall distribution. *ANZIAM Journal*, 51, C231–C246.

Zhaoxia, R., Dayuan, Y. and Yuebo, X. (2003) Droughts, flood disasters, and climate change during the last 2000 years in Heihe River basin. XVI INQUA CONGRESS. Shaping the Earth: A Quaternary Perspective. Paleoseismology in the Twenty-first Century, a Global Perspective, July 23-30, Reno, Nevada, USA.